Journal of Electroanalytical Chemistry 819 (2018) 78–86

Contents lists available at ScienceDirect

Journal of Electroanalytical Chemistry

journal homepage: www.elsevier.com/locate/jelechem

Distribution potential in electrified microemulsions with potential determining salts

José A. Manzanares[a,*], Christoffer Johans[b,1], Javier Cervera[a]

[a] Department of Thermodynamics, Faculty of Physics, University of Valencia, E-46100 Burjasot, Spain
[b] Department of Chemistry, School of Chemical Engineering, Aalto University, P.O. Box 16100, FI-00076 Aalto, Finland

ARTICLE INFO

Keywords:
Distribution potential
Potential determining salt
Microemulsion
ITIES
Electroneutrality
Poisson-Boltzmann equation

ABSTRACT

The electrical polarization of lamellar and water-in-oil microemulsions composed of the aqueous solution of a potential determining salt (PDS), an organic solvent and a nonionic surfactant has been studied. The distribution of the PDS ions across the interface between two immiscible electrolyte solutions (ITIES) generates an electrical potential difference which can be used to control charge transfer processes. In macroscopic ITIES, this distribution potential is independent of the PDS concentration and can be determined from the electroneutrality condition far from the interface. In microemulsions, on the contrary, the distribution potential is smaller in magnitude and depends on the PDS concentration, the surfactant concentration and, in principle, the microemulsion (geometrical) structure. This different behaviour appears because the interfacial area per volume is so large that the charge needed to establish the macroscopic distribution potential exceeds the total charge present in the system, and hence large deviations from local electroneutrality occur in the whole microemulsion.

1. Introduction

In liquid-liquid electrochemistry, potential determining salts (PDSs) have long been used to apply electrical potential differences without electrodes [1,2]. These salts are formed by ions with different hydrophobicity [3]. The equilibrium redistribution of the ions between the phases generates the distribution potential (for a 1:1 PDS) [4–12]

$$\Delta_o^w\phi_\infty = (\Delta_o^w\phi_1^\circ + \Delta_o^w\phi_2^\circ)/2 \quad (1)$$

where $\Delta_o^w\phi_i^\circ \equiv -\Delta G_{tr,i}^{\circ,o\to w}/z_i F$ is the standard transfer potential of ionic species i, z_i is its charge number ($z_1 = -z_2$), $\Delta G_{tr,i}^{\circ,o\to w}$ is its standard Gibbs free energy of transfer from phase o (organic) to w (aqueous), and F is Faraday's constant. Thus, e.g., when the cation is hydrophilic ($\Delta_o^w\phi_+^\circ > 0$) and the anion is hydrophobic ($\Delta_o^w\phi_-^\circ > 0$), the aqueous side of the electrical double layer has an excess of positive charge, $\Delta_o^w\phi_\infty > 0$. The distribution potential can range between -0.7 V and $+0.7$ V for some PDSs.

Microemulsions are thermodynamically stable mixtures of two immiscible solvents and, at least, one amphiphilic component [13,14]. Their solubilization capacity and very high interfacial area per volume are exploited in many applications. The growing interest in microheterogeneous media has prompted the development of microemulsions suited for electrochemical reactions [15]. For instance, the spatial confinement of reactions in colloidal solutions and microemulsions enables the size control in the synthesis of metal nanoparticles [16,17].

Microemulsions with PDSs are essential in the development of photoionic cells for conversion of solar energy to redox fuels that can be discharged in a flow cell to generate electricity on demand [18,19]. In photovoltaic cells the generated electron-hole pairs are separated by an electric field. In photoionic cells the charge separation takes place at the ITIES (interface between two immiscible electrolyte solutions). Upon light adsorption, the excited dye is quenched in the aqueous phase to form both an oxidized quencher and a reduced neutral dye that partitions to the organic phase. The specificity of a photoionic cell stems from the presence of an electrochemical potential gradient at a liquid–liquid interface arising from a difference of solvation energy of the different species. A key issue for efficiency is that the biphasic system should be emulsified to increase the contact area between phases, ensure a fast extraction reaction and avoid the recombination. The partition of ionic species through the liquid–liquid interface can be controlled by adjusting the distribution potential using PDSs [20–24].

Microemulsions with PDSs have several distinctive features that make them different from macroscopic ITIES and from ordinary microemulsions, either with ionic or nonionic surfactants. First, the dissociated ions accumulate at both sides of the interface and stabilize the microemulsion, which may be formed even in the absence of surfactant

* Corresponding author.
E-mail address: Jose.A.Manzanares@uv.es (J.A. Manzanares).
[1] Current address: Kibron Inc. Oy Malminkaari 23 A, 00700 Helsinki, Finland.

http://dx.doi.org/10.1016/j.jelechem.2017.08.049
Received 1 July 2017; Received in revised form 22 August 2017; Accepted 24 August 2017
Available online 01 September 2017
1572-6657/

[25]. Second, the distribution potential $\Delta_o^w\phi_\infty$ in a macroscopic ITIES can be established because the available charge is practically unlimited. In microemulsions, the interfacial area per volume is so large that the charge needed to establish $\Delta_o^w\phi_\infty$ across every interface can easily exceed the charge of all the ions present in the system. As a consequence, for the same solvents and PDS, the distribution potential established in microemulsions is smaller than in macroscopic ITIES, $|\Delta_o^w\phi| \leq |\Delta_o^w\phi_\infty|$. Moreover, the distribution potential $\Delta_o^w\phi$ in microemulsions depends on the PDS concentration, the surfactant concentration and, in principle, the microemulsion geometry. Since the charge transfer kinetics in microheterogeneous media is affected by the interfacial potential, the rate of, e.g., proton transfer reactions can be controlled by adjusting $\Delta_o^w\phi$ [24].

The standard description of the distribution potential makes use of the local electroneutrality condition far from the ITIES (i.e., outside the double layer) [8,9]. However, in electrified microemulsions the electrical double layer may span the whole extension of both phases. For example, when a PDS like tetradecylammonium chloride is added to the microemulsion, it has been experimentally verified that the ions partition into different phases so that, for the range of PDS concentrations of practical interest, the hydrophilic chloride anions are located in the aqueous phase and the hydrophobic cations in the organic phase [22].

The importance of the problem of significant deviations from local electroneutrality in small systems has frequently been recognized but its solution has only been derived in the case of small potentials and for nanodroplets in a continuum phase [8,10,11,26,27]. Moreover, while these studies concluded that the distribution potential in small liquid-liquid droplets does not depend on electrolyte concentration [26], experimental results seem to indicate the contrary (under different conditions) [21], and our results in this paper confirm an important dependence of the distribution potential with the electrolyte concentration; the origin of the discrepancy could be in the use of the local electroneutrality condition in the external phase of the small drops [26].

Trapping of ions in different phases and electrical disparity (i.e. absence of electroneutrality) are not phenomena exclusive of electrified microemulsions. For example, a recent development of impact electrochemistry [28,29] uses an oil-in-water emulsion in which the oil nanodroplets trap a highly hydrophobic redox probe [30]. However, electrified microemulsions are exotic systems because the exceptional ability to trap ions (of very different hydrophobicity) in different phases [22] leads to extremely large deviations from local electroneutrality. They have already found interesting applications and may stimulate new electrochemistry.

The objective of this work is to describe the electrical polarization of a microemulsion composed of the aqueous solution of a PDS, an organic solvent and a nonionic surfactant. For this purpose, an efficient framework for the solution of the Poisson-Boltzmann equation (PBE) in different geometries without using the local electroneutrality at any point has to be developed. This framework is original, although it builds on previous ITIES studies including the effects of the phase volume ratio [31], the deviations from local electroneutrality [26,27,32], as well as studies of colloidal system with ionic surfactants [33]. Our results are important for the several applications of electrified emulsions mentioned above, as well as for other (nanoscale) electrochemical systems with large deviations from electroneutrality. The emphasis is placed on providing physical insights that stimulate further experimental work based on the control of a variable distribution potential.

2. Theoretical modelling of the distribution potential in microemulsions

2.1. Cell dimensions as determined from the microemulsion composition

The aqueous solution of a PDS, a nonionic surfactant, and an organic solvent (that initially contains no dissolved electrolyte) are considered as three pseudocomponents of the microemulsion, with volume fractions Φ_w, Φ_s and Φ_o. For the sake of clarity, we restrict to the intersection of the $\Phi_w = \Phi_o$ plane and a constant temperature plane of the microemulsion phase prism. For Φ_s higher than that of the $\widetilde{X}$ point of the microemulsion, where the three-phase body meets the one phase region (i.e., in the tail of Kalhweit's fish phase diagram) [13,22], an increase in temperature produces a phase change from o/w microemulsion (oil swollen micelles in aqueous continuous phase) to lamellar structure, and then to w/o microemulsion (water-in-oil or swollen reverse micelles). We consider here the lamellar and w/o microemulsions, and explain the dependence of $\Delta_o^w\phi$ on the nature and concentration of the PDS, the surfactant concentration, and the geometry of the emulsion microstructure. As usual, it is assumed that phases w and o contain no free surfactant molecules and that the surfactant monolayer contains no ions and solvent molecules.

The structure of the interfacial electrical double layer is determined by solving the Poisson-Boltzmann equation (PBE). For this purpose, the microemulsion is divided in globally electroneutral (spherical or rectangular) cells [34], each consisting of aqueous (w), surfactant (s), and organic (o) phases. The PBE is solved in one cell that extends from $r = 0$ to L, where r is the (radial or axial depending on the microemulsion structure) coordinate normal to the interfaces. Phase w extends from $r = 0$ to L_w, the surfactant monolayer from L_w to $L_w + L_s$, and phase o from $L_w + L_s$ to $L = L_w + L_s + L_o$. The values of L_w, L_o and L are determined in terms of Φ_s and the effective length L_s of the surfactant (headgroup plus tail). In lamellar microemulsions, $L = L_s/\Phi_s$ and $L_w = L_o = L(1 - \Phi_s)/2$. In w/o micelles, the volume of phase j (j = w, s, o) is $V_j = V\Phi_j$ where $V = 4\pi L^3/3$, so that $L_w = L[(1 - \Phi_s)/2]^{1/3}$, $L_w + L_s = L[(1 + \Phi_s)/2]^{1/3}$ and $L = L_s 2^{1/3}/[(1 + \Phi_s)^{1/3} - (1 - \Phi_s)^{1/3}]$.

2.2. Electrical description of the microemulsion

Consider that the PDS is a 1:1 binary electrolyte and denote the more hydrophilic species with subscript 1, $\Delta G_{tr,2}^{\circ,o\to w} > \Delta G_{tr,1}^{\circ,o\to w}$; without loss of generality as $z_1 (= -z_2)$ is still arbitrary. Index k denotes the majority species, i.e. $k = 1$ in phase w and $k = 2$ in phase o, so that the ion concentrations satisfy $c_{1w}(r) \geq c_{2w}(r)$ and $c_{2o}(r) \geq c_{1o}(r)$ and the charge in phases w and o is $Q = Q_w/z_1 = Q_o/z_2 \geq 0$. The majority ions can be called counterions as their excess counterbalance the charge in the opposite phase.

With the coordinate r increasing from phase w to phase o, the electric field satisfies $z_1 d\phi/dr \leq 0$ (Fig. 1). The field and the charge density $\rho_j = F(z_1 c_{1j} + z_2 c_{2j})$ (j = w, o) are large in the vicinity of the surfactant monolayer. Contrarily to macroscopic ITIES, in which the phases are electroneutral beyond some distance (of the order of the Debye length) from the interface, in microemulsions with PDSs the double layer can span the whole phases w and o (because of its nanoscale dimensions) and *local electroneutrality holds nowhere*. The ratios $\alpha_w = c_{2w}(0)/c_{1w}(0) \leq 1$ and $\alpha_o = c_{1o}(L)/c_{2o}(L) \leq 1$ quantify the deviations from electroneutrality at $r = 0$ and L. The Debye parameters are then defined as [35]

$$\kappa_w{}^2 = \frac{F^2 c_{1w}(0)}{2\varepsilon_0\varepsilon_w RT},\ \kappa_o{}^2 = \frac{F^2 c_{2o}(L)}{2\varepsilon_0\varepsilon_o RT} \tag{2}$$

where ε_0 is the permittivity of vacuum and ε_j the relative permittivity of phase j.

The uniformity of the electrochemical potentials of the species i (i = 1, 2) requires

$$c_{iw}(0)\exp[z_i f(\Delta_o^w\phi - \Delta_o^w\phi_i^\circ)] = c_{io}(L) \tag{3}$$

where $f = F/RT$. The mean concentration $c_{\pm j} = [c_{1j}(r)c_{2j}(r)]^{1/2}$ is also independent of position in phase j. The partition coefficient $K_{w/o} = \exp[z_1 f(\Delta_o^w\phi_1^\circ - \Delta_o^w\phi_2^\circ)/2]$ determines the ratio $c_{\pm w}/c_{\pm o}$. In terms of $\xi_{js} = \kappa_j L_j$, the condition $K_{w/o} = c_{\pm w}/c_{\pm o}$ for the distribution equilibrium of the electrolyte can be presented as.

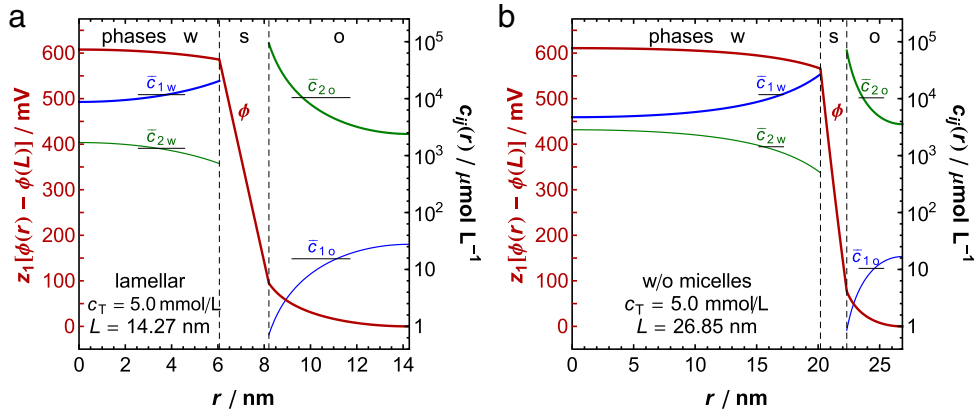

Fig. 1. Equilibrium distribution of the electric potential (left axis, thick line) and ion concentrations (right axis) in a globally electroneutral cell of (a) a lamellar and (b) a w/o water|Tergitol-10|α,α,α–trifluorotoluene microemulsion, with $\Phi_s = 0.15$; in case (b) equal volumes of phases w and o implies that phase o is thinner than the aqueous core. The PDS is lithium tetrakispentafluorophenyl borate ethyl etherate (LiTB) and its concentration referred to the total microemulsion volume is c_T = 5.0 mmol/L. The horizontal seg-ments indicate the average ionic concentrations. Most Li^+ ions (species 1) remain in phase w, and very few transfer to phase o. On the contrary, most TB^- ions (species 2) transfer to phase o and very few remain in phase w. A distribution potential of ca. 610 mV is thus created. A large fraction of this potential drop takes place across the surfactant monolayer. The charge is not localized close to the nonionic surfactant but spans the whole cell. The deviations from electroneutrality are larger at the external boundary of phase o ($r = L$) than at that of phase w ($r = 0$).

$$K_{w/o} = \left(\frac{\alpha_w}{\alpha_o}\right)^{1/2} \frac{\varepsilon_w}{\varepsilon_o} \left(\frac{\xi_{ws} L_o}{\xi_{os} L_w}\right)^2 \tag{4}$$

The ionic concentrations at the cell boundaries can be written as $c_{1w}(0) = c_{\pm w} e^{\varphi_{0w}}$, $c_{2w}(0) = c_{\pm w} e^{-\varphi_{0w}}$, $c_{1o}(L) = c_{\pm o} e^{-\varphi_{0o}}$ and $c_{2o}(L) = c_{\pm o} e^{\varphi_{0o}}$. The microemulsion can then be considered to be in distribution equilibrium with two fictitious, electroneutral solutions with mean concentrations $c_{\pm w}$ and $c_{\pm o}$ and potential difference $\Delta_o^w\phi_\infty$ (Fig. 2). Dividing Eq. (3) for $i = 1$ and 2, it is obtained that $\Delta_o^w\phi_\infty$ can be decomposed in three contributions,

$$\Delta_o^w\varphi_\infty = z_1 f \Delta_o^w\phi_\infty = \varphi_{0o} + z_1 f \Delta_o^w\phi + \varphi_{0w} \tag{5}$$

One is the actual distribution potential $\Delta_o^w\phi = \phi(0) - \phi(L)$ in the microemulsion. The other two are the potential of the fictitious aqueous solution with respect to that at $r = 0$ and the potential of the solution at $r = L$ with respect to the fictitious organic solution (Fig. 2).Their values in RT/z_1F units are $\varphi_{0j} = -(1/2)\ln\alpha_j \geq 0$ (j = w, o).

Compared to macroscopic ITIES, microemulsions have an extremely high surface-to-volume ratio, which increases with Φ_s. In order to create the distribution potential across every interface of the microemulsion, the amount of charge required can easily exceed the total electric charge available, $Q_{max} = Fc_TV$, where c_T is the PDS concentration referred to the total microemulsion volume V. If Q_{max} is not enough to build up $\Delta_o^w\phi_\infty = (\Delta_o^w\phi_1^\circ + \Delta_o^w\phi_2^\circ)/2$, the actual distribution potential $\Delta_o^w\phi$ is smaller in magnitude (Fig. 2) and depends on Φ_s and c_T.

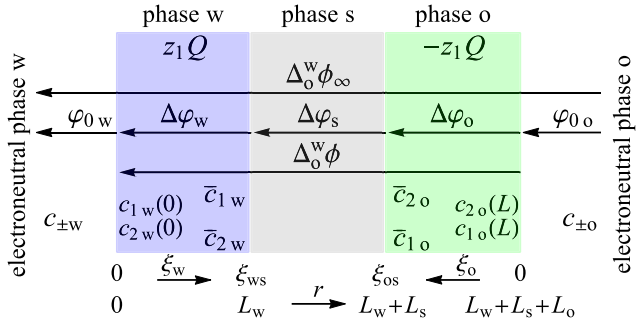

Fig. 2. Schematic representation of the spatial extensions, the ion and electrolyte concentrations, and the potential drops in the microemulsion phases. The distribution potential is the sum of the potential drops in phases w, s and o, $\Delta_o^w\varphi = z_1 f \Delta_o^w\phi = \Delta\varphi_w + \Delta\varphi_s + \Delta\varphi_o$. The potential difference between two fictitious electroneutral solutions in equilibrium with the microemulsion is the distribution potential in macroscopic ITIES, $\Delta_o^w\phi_\infty$. Due to the deviations from electroneutrality at $r = 0$ and L the distribution potential is smaller in the microemulsion, $0 \leq z_1 f \Delta_o^w\phi \leq z_1 f \Delta_o^w\phi_\infty$.

2.3. Poisson-Boltzmann equation (PBE)

Global electroneutrality and symmetry require that the field vanishes at the cell boundaries $r = 0$ and $r = L$, and this fact suggests defining the dimensionless potentials in phases w and o as $\varphi_w(r) = -z_1 f[\phi(r) - \phi(0)] \geq 0$ and $\varphi_o(r) = z_1 f[\phi(r) - \phi(L)] \geq 0$. Inserting $c_{1w}(r) = c_{1w}(0)e^{\varphi_w(r)}$, $c_{2w}(r) = c_{1w}(0)\alpha_w e^{-\varphi_w(r)}$, $c_{2o}(r) = c_{2o}(L)e^{\varphi_o(r)}$ and $c_{1o}(r) = c_{2o}(L)\alpha_o e^{-\varphi_o(r)}$ in the Poisson equation $\nabla^2\phi = -\rho_j/\varepsilon_0\varepsilon_j$, the PBE becomes

$$\frac{d^2\varphi_w}{d\xi_w^2} + \frac{m}{\xi_w}\frac{d\varphi_w}{d\xi_w} = 2(e^{\varphi_w} - \alpha_w e^{-\varphi_w}) \tag{6}$$

$$\frac{d^2\varphi_o}{d\xi_o^2} - \frac{m}{\xi_{oL} - \xi_o}\frac{d\varphi_o}{d\xi_o} = 2(e^{\varphi_o} - \alpha_o e^{-\varphi_o}) \tag{7}$$

where $\xi_w = \kappa_w r$ and $\xi_o = \kappa_o(L - r)$ are the dimensionless position variables, and $\xi_{oL} = \kappa_o L$ (i.e., $\xi_{oL} - \xi_o = \kappa_o r$). The planar and spherical geometries are described simultaneously using the parameter m that takes the values 0 and 2, respectively. The r.h.s. of Eqs. (6) and (7) reduce to $4\sinh\varphi_j$ when $\alpha_j \approx 1$ (i.e., local electroneutrality holds at $r = 0$ and L) and to $2e^{\varphi_j}$ when $\alpha_j \approx 0$ (i.e., almost complete separation of the ion species in different phases). The position variables run from $\xi_j = 0$, where $\varphi_j(0) = 0$ and $d\varphi_j/d\xi_j\,|_{\xi_j = 0} = 0$, to $\xi_{js} = \kappa_j L_j$, where $\varphi_j(\xi_{js}) = \Delta\varphi_j$ and the field is

$$\left.\frac{d\varphi_j}{d\xi_j}\right|_{\xi_{js}-} = \frac{2f\,Q}{\xi_{js} C_{j0}} (j = w, o) \tag{8}$$

In Eq. (8), $C_{j0} = 2\varepsilon_0\varepsilon_j A_j/L_j$ and A_j is the area of the interface between phases s and j; for w/o micelles, $A_w = 4\pi L_w{}^2$ and $A_o = 4\pi(L - L_o)^2$.

In the surfactant monolayer the PBE reduces to the Laplace equation, $\nabla^2\phi = 0$, because no ions are present, so that $\phi(r) - \phi(L_w) = (\Delta\phi_s/L_s)(r - L_w)[(L_w + L_s)/r]^{m/2}$ and the potential drop is

$$\Delta\varphi_s = z_1 f\,[\phi(L_w) - \phi(L - L_o)] = f\,Q/C_s \tag{9}$$

where $C_s = \varepsilon_0\varepsilon_s(A_wA_o)^{1/2}/L_s$ is the electrical capacitance of this layer.

The major hurdle in the description of systems where local electroneutrality holds nowhere is that the ionic concentrations are not known at any point [32]. The PBE can become highly nonlinear in some cases, and the potential profile is then extremely sensitive to the values α_w and α_o, which are unknown. The problem has a significant mathematical complexity because these parameters vary over many orders of magnitude until they reach $\alpha_j \approx 1$ at high concentrations.

The unknowns parameters α_w, α_o and ξ_{oL} in Eqs. (6) and (7) have to be determined from mass and charge balances. In principle, only the PDS concentration in phase w prior to the microemulsion formation, $c = c_T/\Phi_w$, is known. The mass balance requires (when $\Phi_w = \Phi_o =$

$(1-\Phi_s)/2)$ that

$$\bar{c}_{1w}+\bar{c}_{1o}=c \tag{10}$$

where the overbars denote average value of the ion concentration within the phase. The inequalities $\bar{c}_{1w}>\bar{c}_{2w}$ and $\bar{c}_{2o}>\bar{c}_{1o}$ hold because species 2 is more hydrophobic than species 1 (Fig. 1). Lower bounds of α_j can be found from Eq. (3). In the limit $c\to 0$, $c_{1w}(0)\approx\bar{c}_{1w}$ and $c_{2o}(L)\approx\bar{c}_{2o}$ because the potential drops $\Delta\varphi_j$ are negligible, and $\bar{c}_{1w}=c=\bar{c}_{2o}$ from Eq. (10) because the minority ions are excluded. Hence, Eq. (3) implies $\lim_{c\to 0}\alpha_o=\exp(-z_1 f\Delta_o^w\phi_1^\circ)$ and $\lim_{c\to 0}\alpha_w=\exp(-z_1 f\Delta_o^w\phi_2^\circ)$; which are equivalent to $\lim_{c\to 0}(\alpha_w/\alpha_o)^{1/2}=K_{w/o}$ and $\lim_{c\to 0}(\alpha_w\alpha_o)^{1/2}=\exp(-z_1 f\Delta_o^w\phi_\infty)$.

A practical solution procedure considers ξ_{os} as the independent variable (instead of c), for this choice also determines $\xi_{oL}=\xi_{os}L/L_o$, and ξ_{ws} becomes a function of α_w and α_o from Eq. (4). Initial guesses of α_w and α_o are used to solve the PBE; for low ξ_{os}, $\alpha_w\approx\exp[z_1 f(\Delta_o^w\phi-\Delta_o^w\phi_2^\circ)]$ and $\alpha_o\approx\exp[z_1 f(\Delta_o^w\phi-\Delta_o^w\phi_1^\circ)]$. The values of α_w and α_o are then iteratively adjusted until two conditions are satisfied: (i) the charge Q in Eq. (8) for phase w is the same as for phase o, and (ii) the distribution potential $z_1 f\Delta_o^w\phi=\Delta\varphi_o+\Delta\varphi_s+\Delta\varphi_w$ satisfies Eq. (5), $(\alpha_w\alpha_o)^{1/2}=\exp[z_1 f(\Delta_o^w\phi-\Delta_o^w\phi_\infty)]$. The concentrations $c_{1w}(0)=2\varepsilon_0\varepsilon_w RT(\xi_{ws}/FL_w)^2$, $c_{2w}(0)=\alpha_w c_{1w}(0)$, $c_{1o}(L)=\alpha_o c_{2o}(L)$ and $c_{2o}(L)=2\varepsilon_0\varepsilon_o RT(\xi_{os}/FL_o)^2$ are then known. The average concentrations $\bar{c}_{1w}$ and $\bar{c}_{2o}$ are calculated from

$$\bar{\xi}_{1w}^{\,2}\equiv\frac{F^2\bar{c}_{1w}L_w^{\,2}}{2\varepsilon_0\varepsilon_w RT}=\frac{m+1}{\xi_{ws}^{m-1}}\int_0^{\xi_{ws}}e^{\varphi_w}\xi_w^{\,m}d\xi_w \tag{11}$$

$$\bar{\xi}_{2o}^{\,2}\equiv\frac{F^2\bar{c}_{2o}L_o^{\,2}}{2\varepsilon_0\varepsilon_o RT}=\frac{(m+1)\xi_{os}^{\,2}}{\Phi_o\xi_{oL}^{m+1}}\int_0^{\xi_{os}}e^{\varphi_o}(\xi_{oL}-\xi_o)^m d\xi_o \tag{12}$$

The concentrations $\bar{c}_{1o}$ and $\bar{c}_{2w}$ of the minority ions, also known as stoichiometric electrolyte concentrations [33,36], are determined from the known Q and the charge balance, $Q/FV\equiv\Phi_w(\bar{c}_{1w}-\bar{c}_{2w})=\Phi_o(\bar{c}_{2o}-\bar{c}_{1o})$. Finally, the PDS concentration c is determined from Eq. (10) for either $i=1$ or 2.

The PBE in spherical geometry has no analytical solution for the situation of interest here, with large deviations from local electroneutrality. These deviations make useless to work out approximate solutions using linearization techniques. Series expansions [32,33] are not valid either because for every value of α_j in Eqs. (6) and (7) the potential φ_j diverges at a critical value of ξ_j associated with the phenomenon of (counterion) condensation and the number of terms in the series always becomes insufficient for some concentration. Approximate analytical solutions of Eq. (7) exist for $\alpha_o\approx 0$ [37,38]. Interestingly, even when the charge and the distribution potential are large, the region furthest from the surfactant in phase o has a uniform space charge density [39].

2.4. Differential capacitance and polarization regimes

The differential electrical capacitance of the cell is [40,41]

$$\frac{1}{C}\equiv\frac{1}{z_1}\frac{d\Delta_o^w\phi}{dQ}=\frac{1}{f}\left(\frac{d\Delta\varphi_w}{dQ}+\frac{d\Delta\varphi_s}{dQ}+\frac{d\Delta\varphi_o}{dQ}\right)=\frac{1}{C_w}+\frac{1}{C_s}+\frac{1}{C_o} \tag{13}$$

The major contribution to $1/C$ is often due to the surfactant, especially when ε_s is low and the surfactant molecules are relatively long. The capacitance $C_0=\lim_{c_T\to 0}C$ is an important characteristic of the microemulsion because the charge required to establish the distribution potential $\Delta_o^w\phi_\infty$ can be roughly estimated as $Q_{cr}=C_0 z_1\Delta_o^w\phi_\infty$. The associated critical concentration $c_{T,cr}=C_0 z_1\Delta_o^w\phi_\infty/FV$ is proportional to the interfacial area per volume and increases with Φ_s. The electrical polarization of the microemulsion has different characteristics in the regimes $c_T<c_{T,cr}$ and $c_T>c_{T,cr}$; in macroscopic ITIES $c_{T,cr}$ is so small that the regime $c_T<c_{T,cr}$ cannot be observed.

When $c_T<c_{T,cr}$, the solvation energy contribution is dominant and the minimization of the microemulsion free energy is achieved by maximizing the charge separation, $Q\approx Q_{max}=Fc_T V$. The distribution potential $z_1\Delta_o^w\phi$ also increases linearly with c_T as $z_1\Delta_o^w\phi\approx Q/C_0$. Since Q/c_T and $z_1\Delta_o^w\phi/c_T$ take maximum values, we refer to this regime as that of maximum electrical polarization of the microemulsion. The minority ions concentrations $\bar{c}_{1o}$ and $\bar{c}_{2w}$ practically vanish; even though this implies a very low microemulsion entropy (viz., the contribution associated with the ion distribution). The deviations from local electroneutrality at $r=0$ and L are so large that the PBE can be solved using $\alpha_j\approx 0$. The value ξ_{os} determines Q from Eq. (8), and $\bar{c}_{2o}\approx Q/F\Phi_o V$. The charge balance determines ξ_{ws}. The mass balance reduces to $\bar{c}_{1w}\approx\bar{c}_{2o}\approx c$, which is equivalent to $f\,Q/C_{j0}\approx\bar{\xi}_{kj}^{\,2}V_j/A_j L_j$, where $k=1$ if $j=$ w and $k=2$ if $j=$ o; thence, Eqs. (11) and (12) are useless in this regime.

The cell capacitance in the limit $c_T\to 0$ is $C_0\approx(C_{w0}^{-1}+C_s^{-1}+C_{o0}^{-1})^{-1}$. In this limit the space charge density is practically independent of position and the r.h.s. of Eqs. (6) and (7) can be approximated by 2. Thus, $\Delta\varphi_w\approx\xi_{ws}^{\,2}/(m+1)\approx fQ/C_{w0}$ and, hence, $\lim_{c_T\to 0}C_w=C_{w0}$; note that $A_w L_w/V_w=m+1$. Similarly, it is deduced that $\Delta\varphi_o\approx\xi_{os}^{\,2}[L-L_o/(m+1)]/(L-L_o)$ and $fQ/C_{o0}\approx\xi_{os}^{\,2}V_o/A_o L_o$, where $A_o L_o/V_o=1$ in lamellae ($m=0$) and $A_o L_o/V_o=(L-L_o)^2/(L^2-LL_o+L_o^2/3)$ in micelles ($m=2$). Thus, $\lim_{c_T\to 0}C_o=C_{o0}$ in lamellae and $\lim_{c_T\to 0}C_o=C_{o0}'=C_{o0}(L^2-LL_o+L_o^2/3)/[(L-L_o)(L-L_o/3)]$ in micelles. The ratio C_{o0}'/C_{o0} varies from 1 when $\Phi_s\to 1$ to 1.093 when $\Phi_s\to 0$ and, therefore, $C_{o0}'\approx C_{o0}$.

2.5. Exact solution of the PBE in lamellar microemulsions

The PBE can be solved analytically in planar geometry using elliptic functions [42]. The exact solution of Eqs. (6) and (7) in the lamellar case ($m=0$) is

$$\varphi_j(\xi_j)=-2\ln[\mathrm{cd}(\xi_j|\alpha_j)]\quad(j=\mathrm{w,o}) \tag{14}$$

and Eqs. (8), (11) and (12) take the form

$$f\,Q/C_{j0}=(1-\alpha_j)\xi_{js}\,\mathrm{sc}(\xi_{js}\mid\alpha_j)\,\mathrm{nd}(\xi_{js}\mid\alpha_j) \tag{15}$$

$$\bar{\xi}_{kj}^{\,2}=\xi_{js}\int_0^{\xi_{js}}\frac{d\xi_j}{\mathrm{cd}^2(\xi_{js}|\alpha_j)} \tag{16}$$

where $k=1$ if $j=$ w and $k=2$ if $j=$ o. In Eqs. (14)–(16), $\mathrm{cd}(\xi_j\mid\alpha_j)$, $\mathrm{sc}(\xi_j\mid\alpha_j)$ and $\mathrm{nd}(\xi_j\mid\alpha_j)$ are Jacobi elliptic functions of argument ξ_j and parameter α_j [43]. The periodicity of the cd function imposes that $\xi_{js}<\mathrm{K}(\alpha_j)$, where $\mathrm{K}(\alpha_j)$ is the elliptic integral of the first kind. Then, $\alpha_j>\alpha_{j,\min}$ is required when $\xi_{js}>\pi/2$ where $\alpha_{j,\min}$ is defined by $\xi_{js}=\mathrm{K}(\alpha_{j,\min})$. No restriction on α_j exists when $\xi_{js}<\pi/2$ because $\mathrm{K}(\alpha_j)\geq\mathrm{K}(0)=\pi/2$.

Following the solution procedure explained above, ξ_{os} is considered an independent variable and ξ_{ws} a function of α_w and α_o, using Eq. (4). The distribution potential is written as $z_1 f\Delta_o^w\phi=f\,Q(\alpha_o)/C_s-2\ln[\mathrm{cd}(\xi_{ws}\mid\alpha_w)\mathrm{cd}(\xi_{os}\mid\alpha_o)]$ where the function $Q(\alpha_o)=(1-\alpha_o)\xi_{os}\mathrm{sc}(\xi_{os}|\alpha_o)\,\mathrm{nd}(\xi_{os}|\alpha_o)C_{o0}/f$ is defined from Eq. (15). Next, α_w and α_o are determined from $(\alpha_w\alpha_o)^{1/2}=\exp[z_1 f(\Delta_o^w\phi-\Delta_o^w\phi_\infty)]$ and $Q(\alpha_o)=(1-\alpha_w)\xi_{ws}\mathrm{sc}(\xi_{ws}|\alpha_w)\,\mathrm{nd}(\xi_{ws}|\alpha_w)C_{w0}/f$. Finally, $\bar{c}_{1w}$ and $\bar{c}_{2o}$ are obtained from Eq. (16), and c from Eq. (10).

A simpler solution of the PBE can be used in the regime of maximum polarization, $c<c_{cr}$. The charge is then $Q\approx Q_{max}=FcV_w$ and the Jacobi functions with $\alpha_j\to 0$ reduce to trigonometric functions, $\mathrm{cd}(\xi_j\mid\alpha_j)\approx\cos\xi_j$, $\mathrm{sc}(\xi_j\mid\alpha_j)\approx\tan\xi_j$ and $\mathrm{nd}(\xi_j\mid\alpha_j)\approx 1$. Thus, the local potential in phase j is $\varphi_j(\xi_j)=-2\ln(\cos\xi_j)$ and the distribution potential is

$$z_1 f\Delta_o^w\phi=f\,Q/C_s-2\ln(\cos\xi_{ws}\cos\xi_{os}) \tag{17}$$

where ξ_{ws} and ξ_{os} can be found by numerically solving

$$f\,Q/C_{j0} = \xi_{js}\tan\xi_{js} \tag{18}$$

The expression $fQ/C_{j0} \approx 2(\xi_{js}/\pi)^2\{1 + 4/[1 - (2\xi_{js}/\pi)^2]\}$ provides an excellent initial guess of ξ_{js}; note that $\xi_{js} < \pi/2$ in order to avoid the divergence of $\Delta\varphi_j = -2\ln(\cos\xi_{js})$ and fQ/C_{j0}. (The corresponding singularity in $\bar{c}_{kj}$ is associated with the phenomenon of counterion condensation [33].) From Eqs. (4) and (5), the values of α_j can be determined using

$$\alpha_w \approx \exp[z_1 f(\Delta_o^w\phi - \Delta_o^w\phi_2^\circ)]\frac{\xi_{os}\tan\xi_{ws}}{\xi_{ws}\tan\xi_{os}} \tag{19}$$

and $\alpha_o = \exp[2z_1 f(\Delta_o^w\phi - \Delta_o^w\phi_\infty)]/\alpha_w$.

3. Results and discussion

The results presented below correspond to the ethoxylated nonionic surfactant Tergitol-10 ($\varepsilon_s = 3.0$, $L_s = 2.14$ nm) between an aqueous phase ($\varepsilon_w = 78$) and an organic phase of α,α,α–trifluorotoluene (TFT, $\varepsilon_o = 9.3$). The solvents have the same volume fraction, $\Phi_w = \Phi_o$. The PDS is lithium tetrakispentafluorophenyl borate ethyl etherate (LiTB). In this system, $\Delta G_{tr,1}^{\circ,o\to w} = -73.0$ kJ/mol, $\Delta G_{tr,2}^{\circ,o\to w} = 59.5$ kJ/mol, $\Delta_o^w\phi_1^\circ = 756.6$ mV, $\Delta_o^w\phi_2^\circ = 616.7$ mV, $\Delta_o^w\phi_\infty = 686.7$ mV, $f\Delta_o^w\phi_\infty = 26.56$ at 300 K, and $K_{w/o} = 14.97$ [22]. Due to its lower permittivity, the electrical effects are enhanced in the organic phase. The potential drop is larger, the electric field close to the surfactant monolayer is larger, the exclusion of the minority ions is more effective, and the deviations from local electroneutrality are larger in phase o than in phase w.

Interestingly, the microemulsion geometry only implies minor differences in the electrical double layer structure. For instance, for $c_T = 5.0$ mM the distribution potential is ca. 610 mV in both geometries (Table 1 and Fig. 1), to be compared with the macroscopic value $\Delta_o^w\phi_\infty = 686.7$ mV. The charge $Q/FV \approx 4.3\text{mM} \lesssim c_T = Q_{max}/FV$ and the average ionic concentrations in phases w and o are also very similar in the two geometries (Table 1).

In liquid-liquid electrochemistry, the distribution potential $\Delta_o^w\phi_\infty$ is defined from the standard Gibbs free energy of transfer of the ions and is independent of the electrolyte concentration, Eq. (1). On the contrary, the distribution potential $\Delta_o^w\phi$ in microemulsions with PDSs depends on the PDS concentration c_T. At low c_T, $\Delta_o^w\phi$ increases almost linearly with c_T (Fig. 3 insets). Its contributions $\Delta\varphi_w \approx fQ_{max}/C_{w0}$, $\Delta\varphi_s \approx fQ_{max}/C_s$ and $\Delta\varphi_o \approx fQ_{max}/C_{o0}$ also increase linearly with c_T, while $\varphi_{0w} = -(1/2)\ln\alpha_w$ and $\varphi_{0o} = -(1/2)\ln\alpha_o$ decrease linearly with c_T. At larger concentrations, a deviation from these linear behaviours occurs because the approximations $C_w \approx C_{w0}$ and $C_o \approx C_{o0}$ no longer hold. Above the critical concentration, $c_T > c_{T,cr}$, $\Delta_o^w\phi$ increases asymptotically toward the macroscopic value $\Delta_o^w\phi_\infty$ and eventually becomes independent of c_T (Fig. 3).

The difference between the actual distribution potential and its macroscopic value is due to the deviations from electroneutrality at $r = 0$ and L, $\Delta_o^w\varphi_\infty - \Delta_o^w\varphi = \varphi_{0w} + \varphi_{0o}$. These deviations are larger in phase o ($r = L$) than in phase w ($r = 0$) and persist well above $c_{T,cr}$, as clearly shown by the importance of the contribution φ_{0o} in the insets of Fig. 3a and b.

The potential drops in the three phases are slightly different when comparing the cases of lamellar and micellar microemulsions (Fig. 3a and b). However, the curves $\Delta_o^w\varphi = \Delta\varphi_o + \Delta\varphi_s + \Delta\varphi_w$ vs. c for the two geometries practically overlap if we superimpose panels 3a and 3b. Similarly, the critical concentration is $c_{T,cr} = C_0 z_1 \Delta_o^w\phi_\infty/FV = 4.091$ mM in the lamellar case and $c_{T,cr} = 4.084$ mM in the micellar case. The lack of influence of the microemulsion geometry on some of its electrical properties occurs because $V/(A_wA_o)^{1/2} \approx L_s/\Phi_s$ in the micellar case and $V/A = L = L_s/\Phi_s$ in the lamellar case and because the areal capacitance of the surfactant monolayer, $C_s/(A_wA_o)^{1/2} \equiv \varepsilon_0\varepsilon_s/L_s = 12.39$ mF/m^2, is a major contribution to C_0 that has the same value in the two geometries.

Below the critical concentration, $c_T < c_{T,cr}$, the solution of the PBE equation in lamellar geometry based on the approximations $\alpha_j \approx 0$ and $Q \approx Q_{max} = FVc_T$, Eqs. (17)–(19), provides a very accurate description of the electrical double layer structure and the contributions to the distribution potential. The exact (either analytical or numerical) solution of the PBE in lamellar and micellar geometries predicts a charge which practically shows no deviation from $Q \approx Q_{max} = FVc_T$ when $c_T < c_{T,cr}$ (Fig. 4a).

Above the critical concentration, this approximation no longer holds and the exact PBE must be solved to describe the tendency of the distribution potential toward its macroscopic value, Eq. (1). At high enough concentrations, the distribution potential reaches its macroscopic value $\Delta_o^w\phi = \Delta_o^w\phi_\infty$, but the charge Q and $\Delta\varphi_s$ continue to increase with c (Fig. 4b) while $\Delta\varphi_w$ and $\Delta\varphi_o$ decrease with c (Fig. 3). The Gouy-Chapman equation $d\varphi_j/d\xi_j|_{\xi_{js}-} = 4\sinh(\Delta\varphi_j/2)$, or

$$f\,Q/C_{j0} = 2\xi_{js}\sinh(\Delta\varphi_j/2) \tag{20}$$

helps to understand these dependencies with c when $c \gg c_{cr}$. The charge Q is determined from macroscopic distribution potential

$$z_1 f\Delta_o^w\phi_\infty = f\,Q/C_s + 2\text{arsinh}(f\,Q/2C_{w0}\xi_{ws}) + 2\text{arsinh}(f\,Q/2C_{o0}\xi_{os}) \tag{21}$$

where $\xi_{js} = \kappa_j L_j$ for j = w and o are calculated using $c_{2o}(L) \approx c/(1 + K_{w/o})$ and $c_{1w}(0) \approx K_{w/o}c_{2o}(L)$. Since $C_{j0}\xi_{js}$ is proportional to $c^{1/2}$, $\Delta\varphi_j$ decreases with c while Q increases with c more slowly than $c^{1/2}$. Note that Eq. (20) is based on the local electroneutrality approximation at $r = 0$ and L, $1 - \alpha_j \ll 1$, which is a very good approximation for phase w and rather good for phase o when $c \gg c_{cr}$.

The major implication of the microemulsion geometry (lamellar or micellar) is that the thickness of the aqueous and organic phases are very different. For $\Phi_s = 0.15$ and $L_s = 2.14$ nm, the cell dimensions are $L_w = L_o = 6.06$ nm and $L = 14.27$ nm in the lamellar microemulsion, and $L_w = 20.19$ nm, $L_o = 4.52$ nm and $L = 26.85$ nm in the w/o micelles. These dimensions are similar to the Debye length (observe that $\xi_{js} = \kappa_j L_j \approx 1$ in Table 1), which implies that the electrical double layer extends over the whole cell. Because $L_w^{mic} > L_w^{lam}$, the deviations from local electroneutrality at $r = 0$ are smaller in the micellar case, $\alpha_w^{mic} > \alpha_w^{lam}$, and the Debye length is slightly shorter in the micellar phase w as $c_{1w}^{mic}(0) > c_{1w}^{lam}(0)$. Similarly, $L_o^{mic} < L_o^{lam}$ implies that deviations from local electroneutrality at $r = L$ are larger in the micellar case, $\alpha_o^{mic} < \alpha_o^{lam}$, and that the Debye length is slightly larger in the micellar phase o. These geometrical effects enhance the electrical effects mentioned above and, therefore, we can conclude that $\alpha_w^{mic} > \alpha_w^{lam} >> \alpha_o^{lam} > \alpha_o^{mic}$ for a wide concentration range (Fig. 4b), which is useful to know when solving the PBE in this complex situation. At the critical concentration α_w gets close to one, but α_o is significantly smaller than one well above the critical concentration, which indicates that deviations from local electroneutrality persist in phase o. The limit $\alpha_o \to 1$ can hardly be achieved because of the solubility limit of the PDS.

Table 1
Ionic concentrations (in mmol/L), contributions to the distribution potential and related variables in water|Tergitol-10|TFT microemulsions with $\Phi_s = 0.15$ and $c_T = 5.0$ mmol/L ($c = c_T/\Phi_w = 11.765$ mmol/L) LiTB (see Fig. 1). The distribution potential $f\Delta_o^w\phi = \varphi_{0w} + \Delta\varphi_w + \Delta\varphi_s + \Delta\varphi_o + \varphi_{0o}$ is very similar in the lamellar and w/o micellar geometries and is smaller than the macroscopic value $f\Delta_o^w\phi_\infty = 26.56$ ($\Delta_o^w\phi_\infty = 686.7$ mV).

Lamellar		Micellar	
$\bar{c}_{1w} = 11.750$	$\bar{c}_{1o} = 0.015$	$\bar{c}_{1w} = 11.754$	$\bar{c}_{1o} = 0.010$
$\bar{c}_{2w} = 1.342$	$\bar{c}_{2o} = 10.423$	$\bar{c}_{2w} = 1.429$	$\bar{c}_{2o} = 10.335$
$Q/FV_w = 10.408$	$Q_{max}/FV_w = 11.765$	$Q/FV_w = 10.325$	$Q_{max}/FV_w = 11.765$
$c_{1w}(0) = 8.756$	$c_{2o}(L) = 2.396$	$c_{1w}(0) = 4.722$	$c_{2o}(L) = 3.562$
$\alpha_w = 0.193\,588$	$\alpha_o = 0.011\,539$	$\alpha_w = 0.601\,852$	$\alpha_o = 0.004\,722$
$\xi_{ws} = 0.933\,26$	$\xi_{os} = 1.413\,96$	$\xi_{ws} = 2.281\,75$	$\xi_{os} = 1.285\,89$
$\varphi_{0w} = 0.821$	$\varphi_{0o} = 2.231$	$\varphi_{0w} = 0.254$	$\varphi_{0o} = 2.678$
$\Delta\varphi_w = 0.851$	$\Delta\varphi_o = 3.657$	$\Delta\varphi_w = 1.739$	$\Delta\varphi_o = 2.977$
$\Delta\varphi_s = 19.001$	$\Delta_o^w\phi$/mV = 607.75	$\Delta\varphi_s = 18.914$	$\Delta_o^w\phi$/mV = 610.86

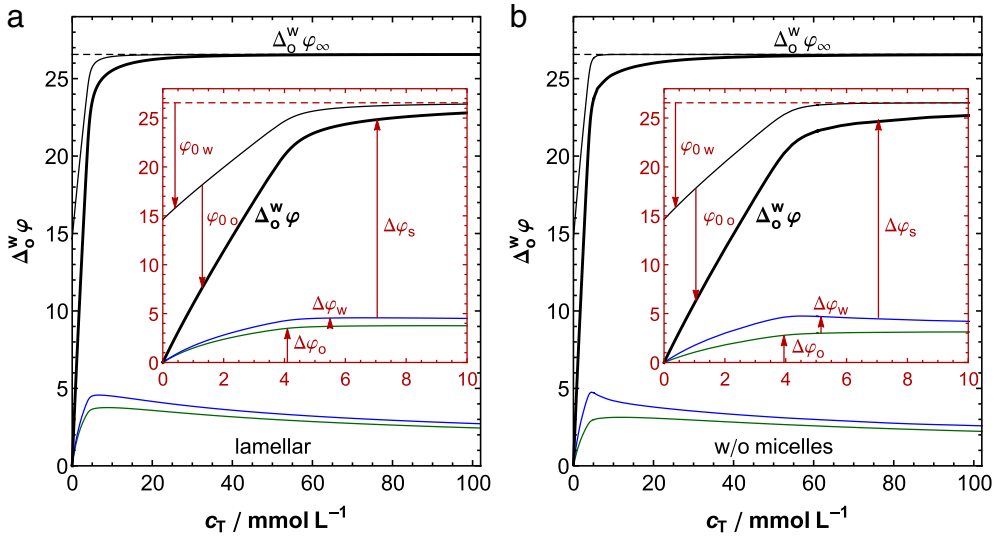

Fig. 3. Distribution potential (thick curve) in (a) a lamellar and (b) a water-in-oil water|Tergitol-10|TFT microemulsion, both with $\Phi_s = 0.15$ and $\Phi_w = \Phi_o$, as a function of the LiTB concentration c_T, referred to the total microemulsion volume. The distribution potential is the sum of the potential drops in the three phases, $\Delta_o^w\varphi = \Delta\varphi_o + \Delta\varphi_s + \Delta\varphi_w$, with $\Delta\varphi_w < \Delta\varphi_o < \Delta\varphi_s$. The insets show magnifications of the concentration range around $c_{T,cr} \equiv C_0 z_1 \Delta_o^w\phi_\infty / FV$.

The minority ions are completely excluded when $c < c_{cr}$, i.e., phase w contains only ionic species 1 and phase o only species 2 [22]. This observation is apparent in the representation of the average concentrations ($\bar{c}_{1w}, \bar{c}_{2w}, \bar{c}_{1o}, \bar{c}_{2o}$) vs. the PDS concentration c (Fig. 5a, inset). The microemulsion reaches then the maximum electrical polarization, $Q \approx Q_{max} = FVc_T = FV_w c$. For high concentrations, ($\bar{c}_{1w}, \bar{c}_{2w}, \bar{c}_{1o}, \bar{c}_{2o}$) are practically linear in c (Fig. 5a), and the lines run in parallel in couples as required by the charge balance $\bar{c}_{1w} - \bar{c}_{2w} = \bar{c}_{2o} - \bar{c}_{1o} = Q/FV_w$ (for $\Phi_w = \Phi_o$) and the fact that Q is almost independent of c when $c \gg c_{cr}$. The average concentrations $\bar{c}_{1w}$ and $\bar{c}_{2w}$ are significantly larger than $\bar{c}_{1o}$ and $\bar{c}_{2o}$ when $c \gg c_{cr}$ because of the value of the partition coefficient $K_{w/o} = c_{\pm w}/c_{\pm o} = 14.97$. Roughly, the slope of the $\bar{c}_{iw}$ vs. c curves is $K_{w/o}/(1 + K_{w/o})$ and that of the $\bar{c}_{io}$ vs. c curves is $1/(1 + K_{w/o})$. However, it should be observed that $K_{w/o}^2 \neq c_{1w}c_{2w}/c_{1o}c_{2o}$ because of the Cauchy-Schwarz-Bunyakovsky inequality, $\bar{c}_{1w}\bar{c}_{2w}/c_{\pm w}^2 = \overline{e^{-\varphi_w}}\;\overline{e^{\varphi_w}} \geq 1$ and $\bar{c}_{1o}\bar{c}_{2o}/c_{\pm o}^2 = \overline{e^{-\varphi_o}}\;\overline{e^{\varphi_o}} \geq 1$ [35,44]. The ratio $\bar{c}_{1o}\bar{c}_{2o}\ c_{\pm o}^2$ is much larger than $\bar{c}_{1w}\bar{c}_{2w}/c_{\pm w}^2$ because $\Delta\varphi_o > \Delta\varphi_w$ (due to their lower permittivity of phase o); in Fig. 5a, $\bar{c}_{1o}\bar{c}_{2o}/c_{\pm o}^2 = 2.51$, 2.33 and 1.91 at $c = 20$, 40 and 80 mmol/L, respectively. The inequality $\bar{c}_{1o}\bar{c}_{2o} \geq c_{\pm o}^2$ can also be observed in Table 1 and in Fig. 1, where it can be appreciated that the position r_1 at which $c_{1o}(r_1) = \bar{c}_{1o}$ differs from r_2 at which $c_{2o}(r_2) = \bar{c}_{2o}$ so that $\bar{c}_{2o} = c_{2o}(r_2) > c_{2o}(r_1) = c_{\pm,o}^2/c_{1o}(r_1) = c_{\pm,o}^2/\bar{c}_{1o}$.

The lamellar or micellar microemulsion geometry affects the ion concentration distributions (Fig. 1) and hence the concentrations at the cell boundaries $r = 0$ and L. The curves that represent $(c_{1w}(0), c_{2w}(0), c_{1o}(L), c_{2o}(L))$ vs. the PDS concentration c are different for lamellar or micellar microemulsions (Fig. 5b). The minority ions are excluded, $c_{2w}(0) \approx c_{1o}(L) \approx 0$, when $c < c_{cr}$. Both microemulsion geometries satisfy $c_{1w}(0) \approx c_{2w}(0) \lesssim c$, $c_{1o}(L) \approx c_{2o}(L)$ and $c_{1w}(0) \approx I_{u\text{-}o} c_{2o}(L)$ when $c \gg c_{cr}$.

The macroscopic distribution potential is a potential difference between two phases of different composition and, hence, not measurable from a thermodynamics point of view. However, the conventions established in liquid-liquid electrochemistry make possible to evaluate the standard Gibbs free energies of transfer of the ions, their standard potentials, and hence the distribution potential, from experimental results. The measurement of the distribution potential in microemulsions is much more difficult experimentally. Our results show that, below the critical concentration, the distribution potential increases with the PDS concentration (Fig. 3) and decreases with increasing surfactant volume fraction (Fig. 6), as an increase of Φ_s involves larger area-to-volume ratio and larger capacitance, Eq. (13). The only experimental results available for the distribution potential in microemulsions [21,22] are in qualitative agreement with the predictions of our theoretical modelling. It should be noted, however, that every model involves a number of simplifying assumptions. For instance, the rate of variation of the distribution potential with the PDS concentration is roughly proportional to L_s^2 (Fig. 6) at low concentrations, and the effective value of L_s (as well as the effective relative permittivity ε_s) may be affected by the penetration of ions or solvent molecules in the surfactant monolayer, which has been neglected.

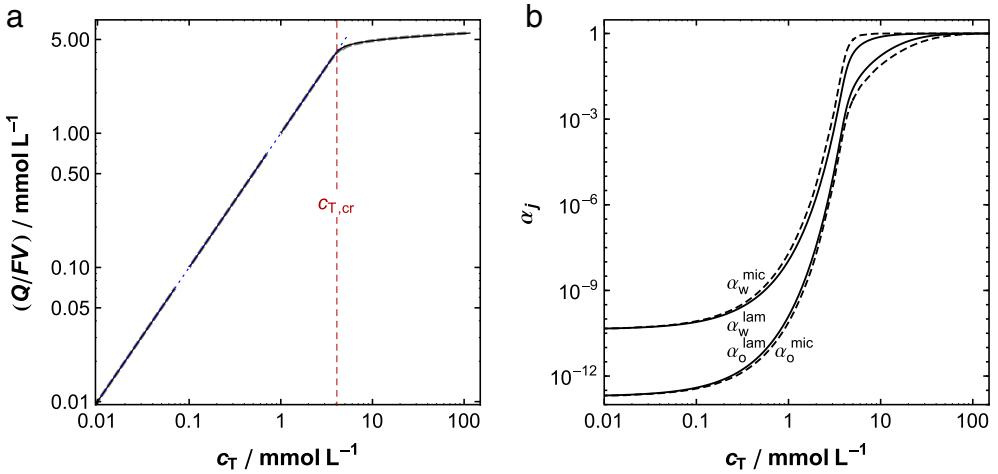

Fig. 4. (a) Below the critical concentration, the solubilization of the PDS in the microemulsion generates an extraordinary electrodisparity: cations and anions separate in different phases and the charge takes its maximum value, $Q_{max} = FVc_T$ (dotted line). At the critical concentration, the charge vs. PDS concentration has a kink and above it the charge continues to slightly increase with concentration without saturation. Lamellar (solid curve) and micellar (dashed, gray curve) microemulsions (with $\Phi_s = 0.15$) have the same charge. (b) The parameters α_j which describe the deviations from local electroneutrality at the cell boundaries $r = 0$ and L vary over more than ten orders of magnitude.

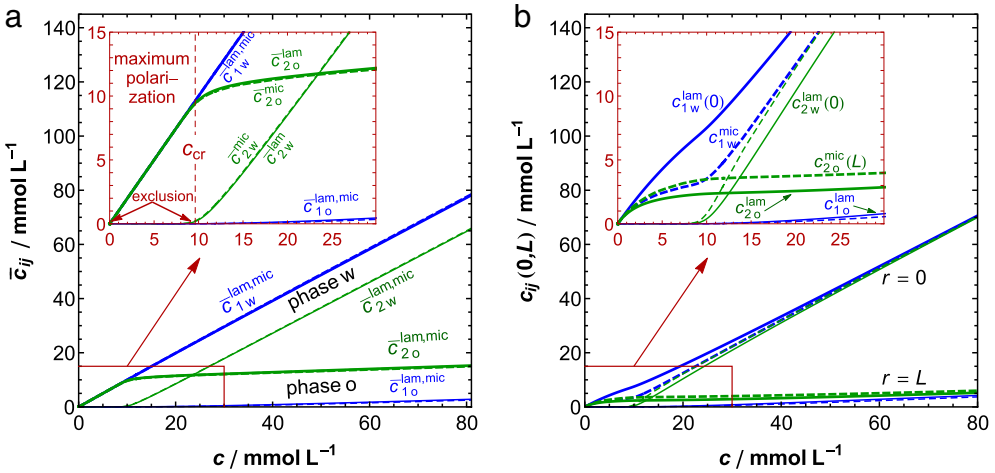

Fig. 5. (a) Average and (b) local (at $r = 0$ and L) ionic concentrations in a lamellar (solid lines) and a water-in-oil (dashed lines) water|Tergitol-10|TFT microemulsion, both with $\Phi_s = 0.15$, as a function of the LiTB concentration c in phase w prior to the microemulsion formation. The thick lines correspond to the majority species (1 in phase w and 2 in phase o) and the thin ones to the minority species. The mass balance $\bar{c}_{1w} + \bar{c}_{1o} = \bar{c}_{2w} + \bar{c}_{2o} = c$ makes convenient the use of c instead of $c_T = c/\Phi_w$ as independent variable. The insets show magnifications. Lamellar and micellar microemulsions have remarkably similar average ionic concentrations (overlapping curves, panel a and inset), in spite of the significant geometrical differences that affect the ion distributions (Fig. 1).

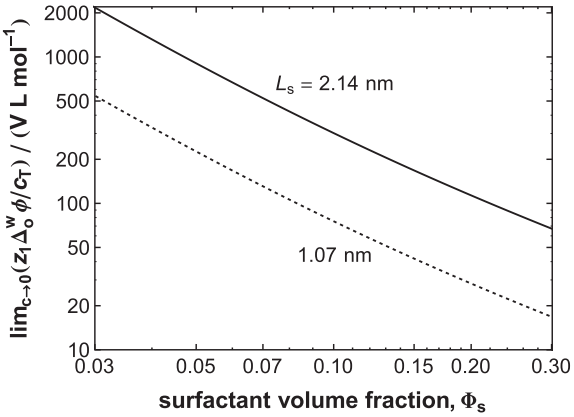

Fig. 6. At low concentrations the distribution potential increases linearly with the PDS concentration. The slope $z_1\Delta_o^w\phi/c_T$ at low concentrations decreases with increasing surfactant volume fraction Φ_s. This slope is roughly proportional to L_s^2, the square of length of the surfactant molecule. The solid curve corresponds to the length Tergitol-10, $L_s = 2.14$ nm. The dotted curve has been calculated with half this value of L_s in order to show that the slope $z_1\Delta_o^w\phi/c_T$ is roughly reduced in a factor 4. The slopes have been calculated for a lamellar microemulsion, but it is expected from previous results that it is practically the same for micellar microemulsions.

4. Conclusions

The distribution potential in lamellar and water-in-oil electrified microemulsions composed of the aqueous solution of a potential determining salt (PDS), an organic solvent and a nonionic surfactant has been studied. Compared to macroscopic ITIES, microemulsions have an extremely high surface-to-volume ratio, which increases with the surfactant volume fraction Φ_s. In order to create the distribution potential across every interface of the microemulsion, the amount of charge required can easily exceed the total electric charge available. When this occurs, the actual distribution potential is smaller in magnitude than in macroscopic ITIES and depends on Φ_s and the PDS concentration c_T.

The charge separation required to build up the distribution potential is determined by its interfacial capacitance. The comparison between the charge available in the microemulsion and the charge required to establish the macroscopic distribution potential $\Delta_o^w\phi_\infty$ determines a critical concentration $c_{T,cr}$ that separates two regimes in relation to the electrical polarization of the microemulsion. In the regime $c_T < c_{T,cr}$, the solvation energy contribution dominates and the minimization of the microemulsion free energy is achieved by maximizing the charge separation. Then, the distribution potential and the charged increase linearly with c_T. In the regime $c_T > c_{T,cr}$, the distribution potential tends asymptotically to its macroscopic value and the solutions become locally electroneutral at the points furthest from the interface, although deviations may persist in the organic phase.

A major complication in solving the PBE in microemulsions where local electroneutrality holds nowhere and the ionic concentrations are not known at any point is that the PBE contains parameters that must be found iteratively from the mass and charge conservation requirements. We have shown that the lamellar or micellar microemulsion geometry has a very minor effect on the distribution potential and the average ionic concentrations in the aqueous and organic phases. This conclusion enables to estimate the electrical properties of micellar microemulsions by using the analytical solution of the Poisson-Boltzmann equation (PBE) in the equivalent lamellar case.

Nomenclature

A_j	interfacial area between phases s and j (= w, o), m^2
C	differential electrical capacitance of cell, F
C_0	$=\lim_{c_T\to 0} C$, F
C_j	differential capacitance of phase j (= w, s, o), F
C_{j0}	$=\lim_{c_T\to 0} C_j$ (except phase o in micelles), F
C'_{o0}	$=\lim_{c_T\to 0} C_o$ in micelles, F
c	$= c_T/\Phi_w$, PDS concentration referred to V_w, mol/m^3
$c_{\pm j}$	mean electrolyte concentration in phase j, mol/m^3
$c_{ij}(r)$	concentration of ionic species i in phase j, mol/m^3
$\bar{c}_{ij}$	average concentration of species i in phase j, mol/m^3
c_T	PDS concentration referred to cell volume, mol/m^3
cd	Jacobi elliptic function cd, 1
f	$= F/RT$, reciprocal of thermal electrical potential, V^{-1}
K	elliptic integral of the first kind, 1
$K_{w/o}$	electrolyte partition coefficient, 1
L	cell dimension, m
L_j	thickness of phase j (= w, s, o), m
m	geometry parameter (value 0 planar, 2 spherical), 1
nd	Jacobi elliptic function nd, 1
PDS	potential determining salt
Q	(absolute) charge separated across interface, C
Q_j	charge in phase j, C
Q_{max}	$= Fc_TV$, upper bound of Q, C
r	position coordinate normal to interfaces, m
sc	Jacobi elliptic function sc, 1
V_j	volume of phase j (j = w, s, o), m^3
V	cell volume, m^3

Greek

α_j	ratio of minority to majority ion concentration at the external boundary of phase j, 1

$\Delta G_{\mathrm{tr},i}^{\circ,\mathrm{o}\to\mathrm{w}}$ standard Gibbs free energy of transfer of i, J/mol
$\Delta\varphi_j$ dimensionless potential drop in phase j, 1
$\Delta_{\mathrm{o}}^{\mathrm{w}}\varphi$ $= z_1 f \Delta_{\mathrm{o}}^{\mathrm{w}}\phi$, dimensionless distribution potential, 1
$\Delta_{\mathrm{o}}^{\mathrm{w}}\phi$ distribution potential, V
$\Delta_{\mathrm{o}}^{\mathrm{w}}\phi_i^{\circ}$ standard transfer potential of ionic species i, V
ε_j relative permittivity of phase j, 1
κ_j Debye parameter in phase j, m^{-1}
ξ_{ij} $= (F^2\bar{c}_{ij}/2\varepsilon_0\varepsilon_j RT)^{1/2} L_j$, 1
ξ_{js} $= \kappa_j L_j$, dimensionless thickness of phase j, 1
ξ_{o} $= \kappa_{\mathrm{o}}(L - r)$, dimensionless position in phase o, 1
ξ_{oL} $= \kappa_{\mathrm{o}} L$, 1
ξ_{w} $= \kappa_{\mathrm{w}} r$, dimensionless position in phase w, 1
ρ_j charge density in phase j, $\mathrm{C/m}^3$
Φ_j volume fraction of phase j (= w, s, o), 1
φ_{0j} $= -(1/2)\ln\alpha_j = z_1 f \phi_{0j}$, 1
φ_{o} $= z_1 f[\phi(r) - \phi(L)]$, dimensionless potential in o, 1
φ_{w} $= -z_1 f[\phi(r) - \phi(0)]$, dimensionless potential in w, 1
ϕ electric potential, V

Subscripts

1 more hydrophilic ion
2 less hydrophilic ion
cr critical, upper bound in maximum polarization regime
k majority ion (1 in phase w, 2 in o)
∞ macroscopic ITIES

Acknowledgements

This work is dedicated to the late Professor Roger Parsons. Financial support from the Ministerio de Economía y Competitividad (MAT2015-65011-P) and European Regional Development Fund through project MAT2015-65011-P is acknowledged.

References

[1] V.J. Cunnane, D.J. Schiffrin, C. Beltran, G. Geblewicz, T. Solomon, The role of phase transfer catalysts in two phase redox reactions, J. Electroanal. Chem. 247 (1988) 203–214, http://dx.doi.org/10.1016/0022-0728(88)80141-4.
[2] P. Peljo, L. Qiao, L. Murtomäki, C. Johans, H.H. Girault, K. Kontturi, Electrochemically controlled proton-transfer-catalyzed reactions at liquid–liquid interfaces: nucleophilic substitution on ferrocene methanol, ChemPhysChem 14 (2013) 311–314, http://dx.doi.org/10.1002/cphc.201200953.
[3] L. Zhang, T. Miyazawa, Y. Kitazumi, T. Kakiuchi, Ionic liquid salt bridge with low solubility of water and stable liquid junction potential based on a mixture of a potential-determining salt and a highly hydrophobic ionic liquid, Anal. Chem. 84 (2012) 3461–3464, http://dx.doi.org/10.1021/ac203425u.
[4] F.M. Karpfen, J.E.B. Randles, Ionic equilibria and phase-boundary potentials in oil-water systems, Trans. Faraday Soc. 49 (1953) 823–831, http://dx.doi.org/10.1039/TF9534900823.
[5] J.A. Manzanares, R.M. Allen, K. Kontturi, Enhanced ion transfer rate due to the presence of zwitterionic phospholipic monolayers at the ITIES, J. Electroanal. Chem. 483 (2000) 188–196, http://dx.doi.org/10.1016/S0022-0728(00)00032-2.
[6] L.Q. Hung, Electrochemical properties of the interface between two immiscible electrolyte solutions: part I. Equilibrium situation and Galvani potential difference, J. Electroanal. Chem. Interfacial Electrochem. 115 (1980) 159–174, http://dx.doi.org/10.1016/S0022-0728(80)80323-8.
[7] L.Q. Hung, Electrochemical properties of the interface between two immiscible electrolyte solutions: part III. The general case of the Galvani potential difference at the interface and of the distribution of an arbitrary number of components interacting in both phases, J. Electroanal. Chem. Interfacial Electrochem. 149 (1983) 1–14, http://dx.doi.org/10.1016/S0022-0728(83)80553-1.
[8] L.Q. Hung, Interfacial potential and distribution equilibria between two immiscible electrolyte solutions, in: A.G. Volkov (Ed.), Interfacial Catalysis, Marcel Dekker, New York, 2003, pp. 83–112 chap. 5 http://dx.doi.org/10.1201/9780203910429.ch5.
[9] V.S. Markin, A.G. Volkov, Potentials at the interface between two immiscible electrolyte solutions, Adv. Colloid Interf. Sci. 31 (1990) 111–152, http://dx.doi.org/10.1016/0001-8686(90)80004-J.
[10] T. Kakiuchi, Limiting behavior in equilibrium partitioning of ionic components in liquid-liquid two-phase systems, Anal. Chem. 68 (1996) 3658–3664, http://dx.doi.org/10.1021/ac960032y.
[11] T. Kakiuchi, Equilibrium electric potential between two immiscible electrolyte solutions, in: A.G. Volkov, D.W. Deamer (Eds.), Liquid-Liquid Interfaces. Theory and Methods, CRC, Boca Raton, 1996, pp. 1–18 (chap. 1).
[12] L. Murtomäki, J.A. Manzanares, S. Mafé, K. Kontturi, Phospholipid at liquid-liquid interfaces and their effect on charge transfer, in: A.G. Volkov (Ed.), Liquid Interfaces in Chemical, Biological and Pharmaceutical Applications, Marcel Dekker, New York, 2001, pp. 533–551 chap. 22 http://dx.doi.org/10.1201/9780203908754.ch22.
[13] H. Wennerström, U. Olsson, Microemulsions as model systems, C. R. Chim. 12 (2009) 4–17, http://dx.doi.org/10.1016/j.crci.2008.08.011.
[14] H. Reiss, H.M. Ellerby, J.A. Manzanares, Configurational entropy of microemulsions: the fundamental length scale, J. Chem. Phys. 99 (1993) 9930–9937, http://dx.doi.org/10.1063/1.465391.
[15] A. Serrà, E. Gómez, G. Calderó, J. Esquena, C. Solans, E. Vallés, Conditions that bicontinuous microemulsions must fulfill to be used as template for electrodeposition of nanostructures, J. Electroanal. Chem. 720–721 (2014) 101–106, http://dx.doi.org/10.1016/j.jelechem.2014.03.033.
[16] J. Hernández, J. Solla-Gullón, E. Herrero, Gold nanoparticles synthesized in a water-in-oil microemulsion: electrochemical characterization and effect of the surface structure on the oxygen reduction reaction, J. Electroanal. Chem. 574 (2004) 185–196, http://dx.doi.org/10.1016/j.jelechem.2003.10.039.
[17] S. Brimaud, C. Coutanceau, E. Garnier, J.-M. Léger, F. Gérard, S. Pronier, M. Leoni, Influence of surfactant removal by chemical or thermal methods on structure and electroactivity of Pt/C catalysts prepared by water-in-oil microemulsion, J. Electroanal. Chem. 602 (2007) 226–236, http://dx.doi.org/10.1016/j.jelechem.2007.01.003.
[18] M.A. Méndez, P. Peljo, M.D. Scanlon, H. Vrubel, H.H. Girault, Photo-ionic cells: two solutions to store solar energy and generate electricity on demand, J. Phys. Chem. C 118 (2014) 16872–16883, http://dx.doi.org/10.1021/jp500427t.
[19] R. Bourdon, P. Peljo, M.A. Méndez, A.J. Olaya, J. De Jonghe-Risse, H. Vrubel, H.H. Girault, Chaotropic agents boosting the performance of photoionic cells, J. Phys. Chem. C 119 (2015) 4728–4735, http://dx.doi.org/10.1021/acs.jpcc.5b00334.
[20] C. Johans, K. Kontturi, Electrochemically driven emulsion inversion, J. Phys. Condens. Matter 19 (2007) 375102, http://dx.doi.org/10.1088/0953–8984/19/37/375102.
[21] S. Vierros, T. Iivonen, C. Johans, Measurement of the potential across the oil-water interface in microemulsion, Electrochem. Commun. 20 (2012) 33–35, http://dx.doi.org/10.1016/j.elecom.2012.03.031.
[22] C. Johans, M. Behrens, K.E. Bergquist, U. Olsson, J.A. Manzanares, Potential determining salts in microemulsions: interfacial distribution and effect on the phase behavior, Langmuir 20 (2013) 15738–157346, http://dx.doi.org/10.1021/la404263v.
[23] V.L. Shapovalov, New charged microheterogeneous system—a microemulsion with droplets of variable electrostatic potential, Russ. Chem. Bull. 41 (1992) 1756–1761, http://dx.doi.org/10.1007/BF00863804.
[24] Yu V. Il'ichev, V.L. Shapovalov, Effect of the electrostatic potential of microemulsion droplets on photoprotolytic dissociation of 1-naphthol, Russ. Chem. Bull. 41 (1992) 1762–1767, http://dx.doi.org/10.1007/BF00863805.
[25] K. Aoki, M. Li, J. Chen, T. Nishiumi, Spontaneous emulsification at oil–water interface by tetraalkylammonium chloride, Electrochem. Commun. 11 (2009) 239–241, http://dx.doi.org/10.1016/j.elecom.2008.11.012.
[26] V.S. Markin, A.G. Volkov, Distribution potential in small liquid-liquid systems, J. Phys. Chem. B 108 (2004) 13807–13812, http://dx.doi.org/10.1021/jp0485385.
[27] Electrical properties of oil/water interfaces, in: A.G. Volkov, V.S. Markin, D.N. Petsev (Eds.), Emulsions: Structure, Stability and Interactions, Elsevier, Amsterdam, 2004, pp. 91–182 chap. 4 http://dx.doi.org/10.1016/S1573-4285(04)80006-1.
[28] J. Ustarroz, M. Kang, E. Bullions, P.R. Unwin, Impact and oxidation of single silver nanoparticles at electrode surfaces: one shot versus multiple events, Chem. Sci. 8 (2017) 1841–1853, http://dx.doi.org/10.1039/c6sc04483b.
[29] P. Peljo, J.A. Manzanares, H.H. Girault, Variation of the Fermi level and the electrostatic force of a metallic nanoparticle upon colliding with an electrode, Chem. Sci. 8 (2017) 4795–4803, http://dx.doi.org/10.1039/C7SC00848A.
[30] H. Deng, J.E. Dick, S. Kummer, U. Kragl, S.H. Strauss, A.J. Bard, Probing ion transfer across liquid-liquid interfaces by monitoring collisions of single femtoliter oil droplets on ultramicroelectrodes, Anal. Chem. 88 (2016) 7754–7761, http://dx.doi.org/10.1021/acs.analchem.6b01747.
[31] Z. Samec, T. Kakiuchi, Effect of the phase volume ratio on the potential of a liquid-membrane ion-selective electrode, Anal. Chem. 76 (2004) 4150–4155, http://dx.doi.org/10.1021/ac0497297.
[32] J.C. Myland, K.B. Oldham, Overcoming electroneutrality: concentrative and electrical conditions inside a charged droplet of electrolyte solution, J. Electroanal. Chem. 522 (2002) 115–123, http://dx.doi.org/10.1016/S0022-0728(02)00686-1.
[33] H.-K. Tsao, Effects of salt addition on the ion distribution enclosed in a cylinder and a sphere, Langmuir 15 (1999) 4981–4988, http://dx.doi.org/10.1021/la981516n.
[34] S. Kuwabara, The forces experienced by randomly distributed parallel circular cylinders or spheres in a viscous flow at small Reynolds numbers, J. Phys. Soc. Jpn. 14 (1959) 527–532, http://dx.doi.org/10.1143/JPSJ.14.527.
[35] T. Gisler, S.F. Schulz, M. Borkovec, H. Sticher, P. Schurtenberger, B. D'Aguanno, R. Klein, Understanding colloidal charge renormalization from surface chemistry: experiment and theory, J. Chem. Phys. 101 (1994) 9924–9936, http://dx.doi.org/10.1063/1.467894.
[36] K. Kontturi, L. Murtomäki, J.A. Manzanares, Ionic Transport Processes, Oxford U. P., Oxford, 2008, pp. 154–164, http://dx.doi.org/10.1093/acprof:oso/9780199533817.003.0004.
[37] F. Oosawa, Polyelectrolytes, Marcel Dekker, New York, 1971, p. 40.
[38] E.K. Zholkovskij, S.S. Dukhin, N.A. Mishchuk, J.H. Masliyah, J. Czarnecki, Poisson–Boltzmann equation for spherical cell model: approximate analytical

solution and applications, Colloids Surf. A Physicochem. Eng. Asp. 192 (2001) 235–251, http://dx.doi.org/10.1016/S0927-7757(01)00728-2.
[39] N. Imai, F. Oosawa, Counter ion distribution around a highly charged spherical polyelectrolyte I (in Japanese), Busseiron Kenkyu 52 (1952) 42–63 http://www.jstage.jst.go.jp/article/busseiron1943/1952/52/1952_52_42/_pdf.
[40] R. Parsons, Thermodynamic methods for the study of interfacial regions in electrochemical systems, in: J.O.M. Bockris, B.E. Conway, E. Yeager (Eds.), Comprehensive Treatise of Electrochemistry, Vol. 1 Plenum Press, New York, 1980chap.1 http://dx.doi.org/10.1007/978-1-4615-6684-7_1.
[41] H.A. Santos, M. Chirea, V. García-Morales, F. Silva, J.A. Manzanares, K. Kontturi, Electrochemical study of interfacial composite nanostructures: polyelectrolyte/gold nanoparticle multilayers assembled on phospholipid/dextran sulfate monolayers at a liquid-liquid interface, J. Phys. Chem. B 109 (2005) 20105–20114, http://dx.doi.org/10.1021/jp052485p.
[42] E.J.W. Verwey, J.Th.G. Overbeek, Theory of the Stability of Lyophobic Colloids, Elsevier, New York, Amsterdam, 1948, pp. 66–76 (chap. 4).
[43] A.J. Brizard, A primer on elliptic functions with applications in classical mechanics, Eur. J. Phys. 30 (2009) 729–750, http://dx.doi.org/10.1088/0143-0807/30/4/007.
[44] J.A. Manzanares, S. Mafé, J. Pellicer, Current efficiency enhancement in membranes with macroscopic inhomogeneities in the fixed charge distribution, J. Chem. Soc. Faraday Trans. 88 (1992) 2355–2364, http://dx.doi.org/10.1039/ft9928802355.